

# Systematic study of the uncertainties in fitting the cosmic positron data by AMS-02

Qiang Yuan<sup>a</sup> and Xiao-Jun Bi<sup>a,1</sup>

<sup>a</sup>Key Laboratory of Particle Astrophysics, Institute of High Energy Physics, Chinese Academy of Sciences, Beijing 100049, P.R. China

E-mail: [yuanq@ihep.ac.cn](mailto:yuanq@ihep.ac.cn), [bixj@ihep.ac.cn](mailto:bixj@ihep.ac.cn)

**Abstract.** The operation of AMS-02 opens a new era for the study of cosmic ray physics with unprecedentedly precise data which are comparable with the laboratory measurements. The high precision data allow a quantitative study on the cosmic ray physics and give strict constraints on the nature of cosmic ray sources. However, the intrinsic errors from the theoretical models to interpret the data become dominant over the errors in the data. In the present work we try to give a systematic study on the uncertainties of the models to explain the AMS-02 positron fraction data, which shows the cosmic ray  $e^+e^-$  excesses together with the PAMELA and Fermi-LAT measurements. The excesses can be attributed to contributions from the extra  $e^+e^-$  sources, such as pulsars or the dark matter annihilation. The possible systematic uncertainties of the theoretical models considered include the cosmic ray propagation, the treatment of the low energy data, the solar modulation, the  $pp$  interaction models, the nuclei injection spectrum and so on. We find that in general a spectral hardening of the primary electron injection spectrum above  $\sim 50 - 100$  GeV is favored by the data. Furthermore, the present model uncertainties may lead to a factor of  $\sim 2$  enlargement in the determination of the parameter regions of the extra source, such as the dark matter mass, annihilation rate and so on.

**Keywords:** dark matter theory, cosmic ray theory

**ArXiv ePrint:** [1408.2424](https://arxiv.org/abs/1408.2424)

---

<sup>1</sup>For correspondence.

---

## Contents

<b>1</b>	<b>Introduction</b>	<b>1</b>
<b>2</b>	<b>Reference configuration</b>	<b>2</b>
<b>3</b>	<b>Systematic uncertainties</b>	<b>5</b>
3.1	Propagation parameters	5
3.2	Low energy data selection	7
3.3	Solar modulation	8
3.4	Other uncertainties	10
3.4.1	Hadronic interaction model	10
3.4.2	Nuclei spectral hardening	11
3.4.3	Versions of GALPROP	12
<b>4</b>	<b>Discussion about the electron spectral hardening</b>	<b>12</b>
<b>5</b>	<b>Conclusion</b>	<b>13</b>

---

## 1 Introduction

One of the biggest discoveries in the cosmic ray (CR) field in recent years is the excess of positrons found by PAMELA<sup>1</sup> [3, 4]. The recent AMS-02 data confirmed PAMELA’s discovery with very high precision and extended the energy range to 350 GeV [5]. The excess positrons require some kinds of “primary” positrons sources [6, 7], either the astrophysical sources like nearby pulsars or exotic sources like dark matter (DM) annihilation or decay. There had been many discussions about the origin of the positron excess in literature (see e.g., the reviews [8–12]).

Thanks to the high precision data from AMS-02, it is possible to perform very detailed study of the properties of the primary positron sources. Following our earlier works on the PAMELA results [13, 14] we gave a quantitative study on the implications of the first AMS-02 positron fraction data in Ref. [15]. In that work we fitted the AMS-02 positron fraction as well as the PAMELA/Fermi-LAT/HESS electron (or total  $e^+e^-$ ) spectra [16–20] to determine the model parameters of both the extra sources and the CR background simultaneously. The fitting shows a tension to explain both the AMS-02 positron fraction and the Fermi total  $e^+e^-$  spectrum simultaneously with the conventional background and extra source model, which works well in the PAMELA era [15]. Such a result was confirmed by several other studies [21–23] and was supported by the AMS-02 preliminary results of the total  $e^+e^-$  spectrum [24].

Although the AMS-02 data are precise enough, the theoretical framework to interpret the data still has large uncertainties, such as the uncertainties from the CR propagation and the solar modulation. In the present work we will give a systematic study of such kinds of uncertainties. Especially we will show how the uncertainties will affect the determination of the model parameters of the extra sources to interpret the data.

---

<sup>1</sup>Actually there were earlier hints on the cosmic positron excesses by HEAT [1] and AMS-01 [2], which did not attract enough attention due to the large errors.

One major uncertainty is the CR propagation. The propagation of CRs in the Galaxy is a diffusive process. The propagation parameters are determined by the secondary-to-primary ratio where the secondaries are generated through interactions between the CRs and the interstellar medium (ISM) during the propagation. However, the propagation parameters, usually determined by the Boron-to-Carbon (B/C) ratio, have relatively large uncertainties [25, 26]. The degeneracy between the propagation parameters is also strong due to the lack of high quality unstable-to-stable ratio of secondaries, such as Beryllium-10 to Beryllium-9 ( $^{10}\text{Be}/^9\text{Be}$ ) ratio. Certainly, with the accumulation of the AMS-02 data the uncertainty of CR propagation is expected to be reduced significantly in future.

Another major uncertainty comes from the complexity of modeling the low energy spectra of the  $e^+e^-$ . The reacceleration or convection during the propagation, as well as the solar modulation, will affect the low energy behavior of the particle spectrum. Sometimes people only select the high energy data (e.g.,  $\gtrsim 10$  GeV) in the studies to avoid the complexity of the low energy spectra [27–30]. However, the results might be biased with limited range of the data. In this work we will show how the results may get affected with different selections of the low energy data. The solar modulation effect will be discussed too with proper approaches to address the uncertainties. Other effects, such as the inelastic hadronic interaction models or the injection proton spectrum, will affect the production of secondary  $e^+e^-$ . They will also be discussed in this work.

The properties of the extra sources themselves should also be a source of uncertainty. For example, the continuous or discrete distribution of the sources [31], and the burst-like or stable injection [32] of the astrophysical sources will give different predictions of the resulting positron spectrum. For the DM scenario, the smooth DM distribution or the local DM clumps will also affect the model parameters to fit the data [33, 34]. In the work we restrict our discussion with continuous source distribution of both the background and the extra source. For the DM annihilation scenario we consider the smooth distribution of the DM in the Milky Way halo and neglect the contribution from DM clumps [35, 36].

The paper is organized as follows. In Sec. 2 we describe the reference configuration as adopted in Ref. [37]. Sec. 3 presents the systematic uncertainties by considering different model configurations. We give some discussion about the results in Sec. 4 and finally give the conclusion in Sec. 5.

## 2 Reference configuration

The reference configuration is adopted following Ref. [37]. It is employed as a benchmark model to compare with different configurations and to illustrate the uncertainties. We briefly describe the major settings of the reference configuration here. The CR propagation is calculated with the public GALPROP package<sup>2</sup>[38], in which the secondary positron flux is predicted through the interaction between the primary CR nuclei and the ISM. The propagation parameters are determined through a fit to the B/C ratio and  $^{10}\text{Be}/^9\text{Be}$  ratio in the diffusion reacceleration (DR) frame. The best fitting propagation parameters are  $D_0|_{R_0=4\text{ GV}} = 5.94 \times 10^{28} \text{ cm}^2 \text{ s}^{-1}$ ,  $\delta = 0.377$ ,  $v_A = 36.4 \text{ km s}^{-1}$  and  $z_h = 4.04 \text{ kpc}$ .

The injection spectrum of the primary electrons are assumed to be a three-piece power-

---

<sup>2</sup><http://galprop.stanford.edu/>

law function with respect to the rigidity,

$$q(R) \propto \begin{cases} (R/R_{\text{br},1}^e)^{-\gamma_0}, & R < R_{\text{br},1}^e \\ (R/R_{\text{br},1}^e)^{-\gamma_1}, & R_{\text{br},1}^e < R < R_{\text{br},2}^e \\ (R/R_{\text{br},2}^e)^{-\gamma_2} (R_{\text{br},2}^e/R_{\text{br},1}^e)^{-\gamma_1}, & R > R_{\text{br},2}^e \end{cases} \quad (2.1)$$

The first break  $R_{\text{br},1}$  is at  $\sim 4$  GV in order to fit the low energy data as well as the radio emission [39], and the second break  $R_{\text{br},2}$  is at  $O(100)$  GV to describe the spectral hardening. We consider two scenarios of the primary electron spectrum: *fittings I* for the cases without spectral hardening at  $O(100)$  GV, and *fittings II* for the cases with a spectral hardening. The number of free parameters of *fittings II* will be larger by 2 (the break rigidity  $R_{\text{br},2}^e$  and the spectral index above it,  $\gamma_2$ ) than that of *fittings I*.

The second hardening of the background electron spectrum<sup>3</sup> was introduced to better fit the AMS-02 positron fraction and the Fermi total  $e^+e^-$  spectrum [21, 27, 37]. Other proposals, like charge asymmetry of the extra source [22, 43], or the multi-component DM model [44], are also discussed to reconcile the tension. The requirement of more electrons at high energies may indicate the effect of discreteness of the primary CR sources [45–47].

The injection spectrum of the primary CR nuclei is adopted to be the same form as shown in Eq. (2.1). The parameters are derived through fitting to the PAMELA [42] and CREAM [41] proton spectra. The secondary electron and positron spectra can then be calculated in the same propagation model. Since we are going to fit the  $e^+e^-$  data, a free scale factor  $c_{e^+}$  is multiplied to the predicted secondary  $e^+e^-$  fluxes. Such a factor is empirical and approximate. It may reflect the possible uncertainties of the overall fluxes of the secondary  $e^+e^-$  fluxes, from e.g., the nuclear enhancement factor, ISM density distribution and so on [48]. Note that those uncertainties may not be exactly recovered by a constant factor [49]. Since the discussion in this work will include the effects of spectral variations due to different propagation models and the hadronic interaction models, we do not employ further degree-of-freedom (dof, such as the form  $c_{e^+}E^p$  adopted in [48]) but keep such a simple re-scale factor, to avoid too much degeneracy of the secondary uncertainties.

Both the astrophysical pulsars and DM annihilation are considered as the extra sources contributing to the  $e^+e^-$  excesses. The spatial distribution of the pulsars is adopted following the pulsar survey [50], and the injection spectrum of  $e^+e^-$  from pulsars is parameterized as a single power-law with an exponential cutoff,  $E^{-\alpha} \exp(-E/E_c)$ . The spectral index  $\alpha$  is limited in the range of  $0.6 - 2.2$  according to Fermi  $\gamma$ -ray observations [51]. The case of multiple components of the pulsar contribution will not be discussed. Actually it has been shown that adding more pulsars do not help to improve the fittings, although it may be physically realistic [52]. The single component can effectively approach the sum of all the pulsars, although without the fine structures [52]. As for the DM scenario, we adopt the annihilation channel  $\tau^+\tau^-$  in this study. The hadronic channels will be constrained by the CR antiproton data [53, 54]. Other leptonic channels, such as  $\mu^+\mu^-$ ,  $4e$ ,  $4\mu$  and  $4\tau$ , may also work to fit the CR lepton data [55]. Given the purpose of this work is to study to what extent the fitting results will be affected by various kinds of systematics, the  $\tau^+\tau^-$  channel is adopted as an illustration (see the Appendix for a comparison of the results for different

---

<sup>3</sup>This was originally motivated by the spectral hardening of CR nuclei around  $\sim 200$  GV by several experiments [40–42]. The most recent AMS-02 data about the proton and Helium spectra show, however, no remarkable structures below  $\sim \text{TV}$  [24]. But the combination of AMS-02 data and CREAM data still shows a spectrum hardening at  $\sim \text{TeV}$ .

annihilation channels). The density profile of DM is adopted to be Navarro-Frenk-White (NFW) distribution [56]. The spatial distribution of the  $e^+e^-$  source does not sensitively affect the propagated results due to the limited propagation lengths of the high energy  $e^+e^-$ .

The solar modulation is treated by the center-force-field approximation [57]. A single modulation potential is assumed for all the leptons in the reference configuration. Since the operation periods between PAMELA/Fermi-LAT and AMS-02 are moderately different in the solar cycle, we will test the case with two different modulation potentials for PAMELA/Fermi-LAT and AMS-02 data, respectively. In some works the charge-sign dependent modulation has been discussed to better describe the data [58–60]. We will also test the charge-dependent modulation effect by employing two different modulation potentials for  $e^+$  and  $e^-$  [61], respectively.

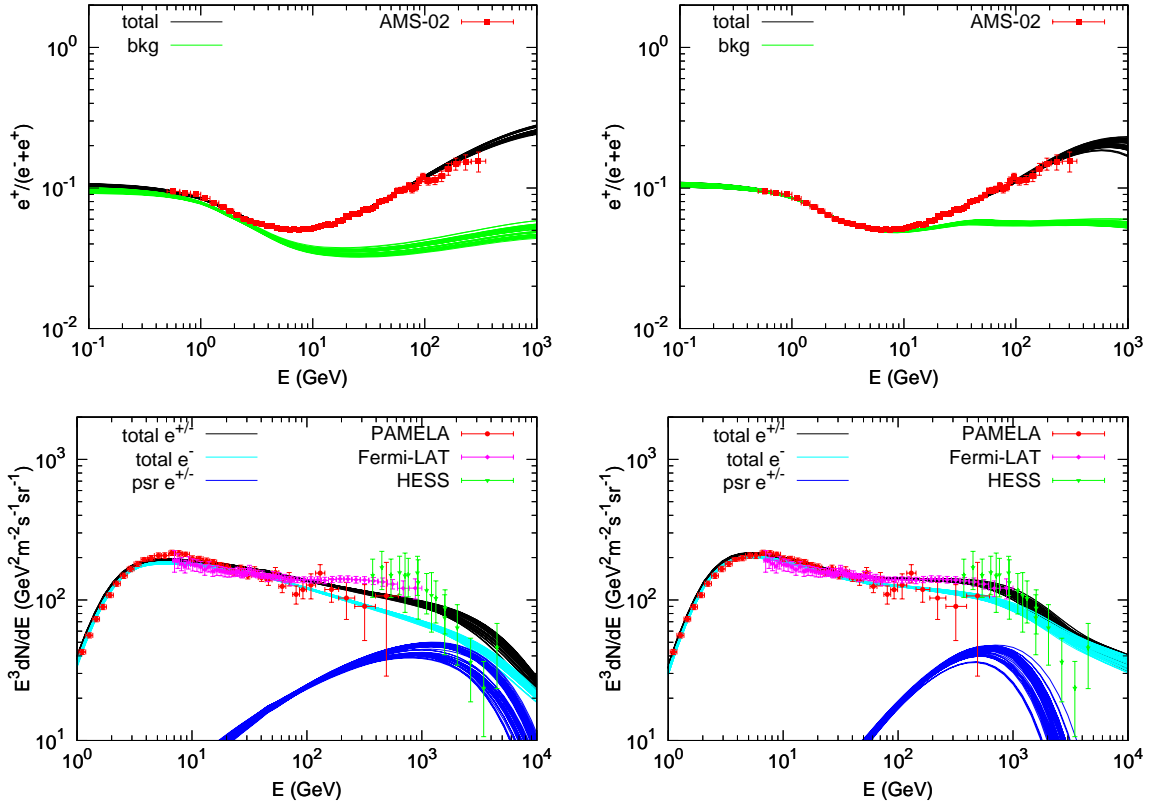


**Figure 1.** The  $2\sigma$  ranges of the positron fraction (upper panels) and electron spectra (lower panels), for 50 randomly selected parameter settings of the reference configuration. The left and right panels are for *fittings I* and *II*, respectively. The pulsars are adopted as the extra sources of the  $e^\pm$ . References of the observational data are: AMS-02 [5], PAMELA [16], Fermi-LAT [18], and HESS [19, 20].

Figure 1 shows the fitting  $2\sigma$  ranges of the positron fraction (upper panels) and electron (or  $e^+e^-$ ) spectra (lower panels), for 50 randomly selected parameter settings of the reference configuration. The left panels are for *fittings I* (without spectral hardening of the primary electrons) and the right panels are for *fittings II*. We can see that *fittings I* seem to underestimate the high energy  $e^+e^-$  fluxes but over-estimate the positron fraction. When a spectral hardening of the primary electron flux is introduced, both the positron fraction and  $e^+e^-$  spectra can be better fitted.

### 3 Systematic uncertainties

In this section we will show the uncertainties when fitting the data by comparing different model settings with the reference configuration. The data used in the fittings include the AMS-02 positron fraction [5], PAMELA electron spectrum [16], Fermi [18] and HESS [19, 20] total electron/positron spectra. The systematic uncertainties of the measurements are added quadratically to the statistical uncertainties.

#### 3.1 Propagation parameters

We first discuss the uncertainties from the propagation parameters. It was found that the DR scenario of CR propagation can well describe the secondary-to-primary ratios of CR nuclei [62, 63]. However, due to the quality of the current CR data, the propagation parameters have relatively large uncertainties [26]. In this work we adopt the six groups of propagation parameters as reported in Ref. [64], which are determined through fitting the B/C ratio for six choices of the propagation halo height  $z_h$  from 2 to 15 kpc. These sets of propagation parameters embrace most uncertainties from the propagation. The values of these parameters are compiled in Table 1.

**Table 1.** Propagation and proton injection parameters

	$D_0^a$ ( $10^{28}\text{cm}^2/\text{s}$ )	$z_h$ (kpc)	$v_A$ (km/s)	$\delta$	$dV_c/dz$ (km/s·kpc)	$A_p^b$	$\gamma_0$	$\gamma_1$	$R_{\text{br},1}$ (GV)	$\gamma_2$	$\Phi_p$ (GV)
1	2.7	2	35.0	0.33	...	4.44	1.76	2.43	15.0	2.37	0.32
2	5.3	4	33.5	0.33	...	4.49	1.79	2.44	13.2	2.37	0.34
3	7.1	6	31.1	0.33	...	4.51	1.82	2.45	12.9	2.37	0.36
4	8.3	8	29.5	0.33	...	4.53	1.86	2.46	14.4	2.37	0.36
5	9.4	10	28.6	0.33	...	4.54	1.87	2.46	14.4	2.38	0.36
6	10.0	15	26.3	0.33	...	4.51	1.89	2.46	16.3	2.37	0.33
7	2.5	4	...	0/0.55 <sup>c</sup>	6	4.60	2.30	2.37	15.7	2.16	0.42
8	5.6	6.5	37.6	0.40	11.1	4.50	1.82	2.43	14.5	2.32	0.31

<sup>a</sup>Diffusion coefficient at  $R = 4$  GV.

<sup>b</sup>Normalization at 100 GeV in unit of  $10^{-9}\text{cm}^{-2}\text{s}^{-1}\text{sr}^{-1}\text{MeV}^{-1}$ .

<sup>c</sup>Below/above  $R = 4$  GV.

It should be noted that the DR scenario is definitely not the only choice to describe the CR propagation. The diffusion plus convection (DC) model could also fit the data moderately [62, 65]. However, a phenomenological break of the diffusion coefficient is needed in order to suppress the low energy B/C ratio [62]. As a comparison, we also take a DC model with parameters given in Ref. [65] in this study. We note that in Ref. [66] the diffusion with both reacceleration and convection (DRC) was shown to be favored, with semi-analytical approach of the CR propagation. We have tested such a model with the B/C and  $^{10}\text{Be}/^9\text{Be}$  data. It shows almost no improvement of the fitting compared with the DR scenario. The possible reason of the difference may come from the difference between the semi-analytical and the full numerical approaches of the CR propagation. Nevertheless, the expectation of the lepton fluxes in the DRC model might be different from the DR or DC models [67]. Therefore we include one example of the DRC model in our discussion to illustrate how the results may be affected.

The best-fitting  $\chi^2$  values for the reference configuration and the above mentioned 8 groups of propagation parameters are summarized in Table 2. From these results we see

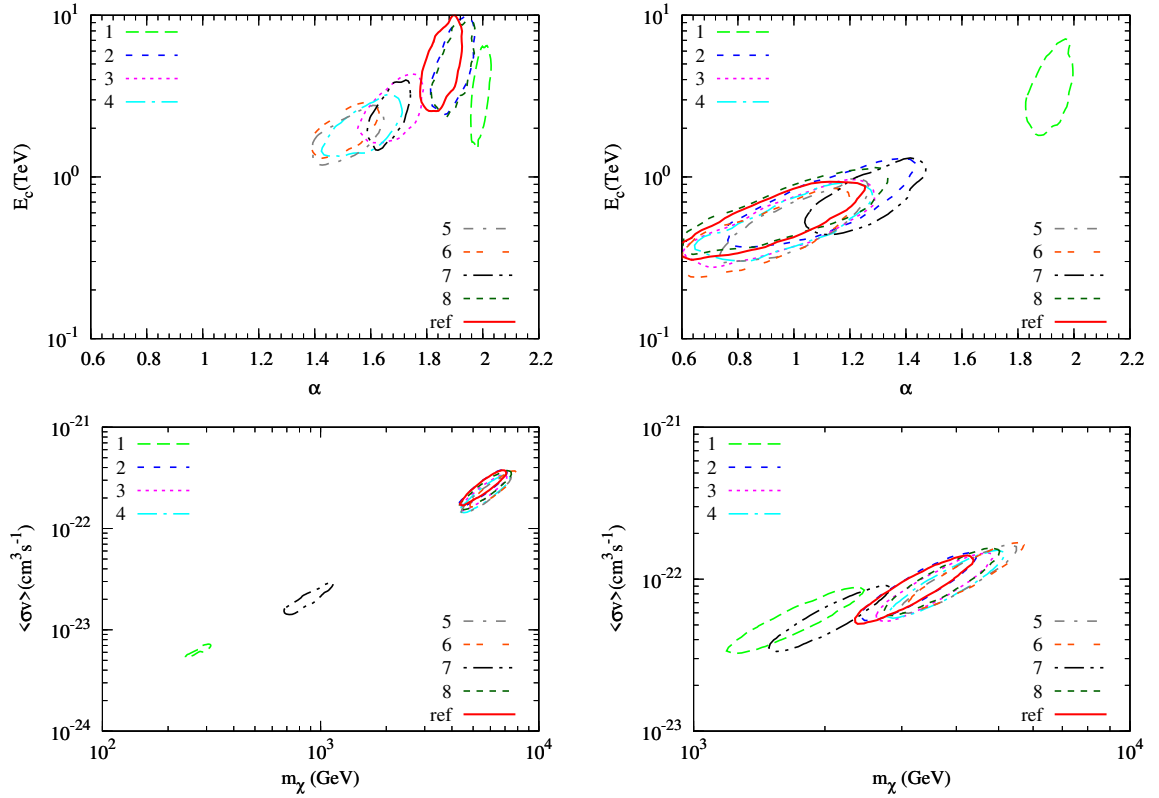


**Figure 2.** Comparison of the  $2\sigma$  confidence regions of  $\alpha - E_c$  in pulsar scenario (top) and  $m_\chi - \langle\sigma v\rangle$  in DM scenario (bottom) for different propagation parameters as given in Table 1. The left (right) panels are for the model without (with) spectral hardening of the primary electrons, i.e., *fittings I* (*II*).

**Table 2.** Fitting  $\chi^2$  for different propagation parameters.

	ref.	1	2	3	4	5	6	7	8
psr-I (166 <sup>a</sup> )	398.2	476.4	344.0	342.3	359.5	378.1	414.9	313.3	369.7
psr-II (164)	134.0	275.4	134.5	146.9	180.6	213.6	239.1	155.4	143.0
DM-I (167)	568.0	1261	570.9	415.9	394.4	395.8	424.8	596.4	588.7
DM-II (165)	133.9	425.9	135.0	149.5	187.0	221.7	252.7	163.6	145.8

<sup>a</sup>In parenthesis is the number of dof.

that in general *fittings I* can hardly fit the data, neither for the pulsar model nor for the DM model. If a spectral hardening of the primary electrons is included (*fittings II*), the fitting results improve significantly. Except for the propagation parameters with extreme values of  $z_h$ , i.e. parameter settings 1, 5 and 6, the reduced  $\chi^2$  values are all smaller or close to 1 for *fittings II*. The results imply strongly that a high energy spectral hardening of the primary electrons is needed. The physical implication of the electron spectral hardening will be discussed later in Sec. IV.

Figure 2 shows the  $2\sigma$  confidence regions on the  $\alpha - E_c$  plane for the pulsar scenario ( $m_\chi - \langle\sigma v\rangle$  plane for the DM scenario). The left panels are for *fittings I* and the right panels



are for *fittings II*. It is shown that for *fittings I* the contours diverse very significant from each other, while for *fittings II* they are more convergent. From Table 2 we can also see that the  $\chi^2$  values for *fittings I* are all too large to be good fittings. It implies that the resulting contours derived in *fittings I* are less statistically meaningful. Nonetheless, the parameters for *fittings II* also have some dispersion among different propagation parameters. It is most remarkable for the parameter setting 1, which actually gives the worst fitting to the data among those parameter settings. For those with acceptable fitting results ( $\chi^2/\text{dof} \sim 1$ ) the favored parameter regions do not differ much. Roughly speaking, the parameter regions of the extra sources may enlarge by a factor of  $\sim 2$  compared with the reference configuration<sup>4</sup>, for reasonable choices of the propagation parameters. Finally, we note that the results of DC and DRC models can be covered by the wide range of the 6 DR models.

### 3.2 Low energy data selection

The low energy part (lower than tens of GeV) of the  $e^+e^-$  spectrum contains very complicated physics because many effects enter in this energy region. The reacceleration/convection, solar modulation and the injection spectral index will all affect the  $e^+e^-$  spectra. At the same time, the measurement uncertainties are the smallest in the low energy range, which contribute significantly to the fittings. As most studies are interested in the properties of the extra sources which contribute to the high energy part, the low energy data below  $\sim 10$  GeV are simply excluded in many works to avoid the complexity. In this subsection, we discuss how the exclusion of the low energy data may affect the conclusions of the study.

**Table 3.** Fitting  $\chi^2/\text{dof}$  for different selections of the data.

	ref.	$E > 5$ GeV	$E > 10$ GeV	$E > 20$ GeV	Fermi ( $E > 70$ GeV)
psr- <i>I</i>	398.2/166	163.5/140	118.7/122	61.0/97	220.7/129
psr- <i>II</i>	134.0/164	110.2/138	89.7/120	48.7/95	75.2/127
DM- <i>I</i>	568.0/167	316.7/141	158.2/123	67.3/98	393.4/130
DM- <i>II</i>	133.9/165	110.3/139	90.2/121	48.7/96	75.5/128

We repeat the fittings of the reference configuration with dropping the data below 5, 10 and 20 GeV and check how the fitting results change. The resulting  $\chi^2$  values are shown in Table 3. We find that the higher the data selection threshold, the smaller the differences between *fittings I* and *II*. For the pulsar scenario with  $E > 5$  GeV, *fittings II* are slightly favored, and for  $E > 10$  and  $E > 20$  GeV cases, both *fittings I* and *II* give acceptable description to the data. Similar conclusion can also be drawn for the DM scenario. Such a result is reasonable because the requirement of a spectral hardening of the primary electrons actually comes from the wide band constraints from the data.

In Ref. [29] since only the data above 20 GeV are employed they can fit all the data without introducing an extra break at primary electron spectrum. This is consistent with our results. The reason should be that the low energy data from PAMELA favors a different electron spectrum from that favored by the Fermi-LAT data. If the low energy data are excluded, there are less constraints from PAMELA, and Fermi-LAT data will dominate the behavior of the background electrons. In this case a single power-law ( $R^{-\gamma_1}$ ) will be enough to fit the data.

<sup>4</sup>Taking the DM scenario for example, the reference configuration gives roughly 2 – 4 TeV for  $m_\chi$ , and it spans  $\sim 1 - 5$  TeV for different propagation models. The constraint on  $m_\chi$  becomes looser by a factor of 2.



Since the low energy  $e^+e^-$  spectra of Fermi-LAT show direct discrepancy with that of PAMELA and AMS-02 [24], we also test the case with only the Fermi-LAT data above  $\sim 70$  GeV. It is shown that dropping the low energy data of Fermi-LAT does not help improve the fitting if no spectral hardening of the primary electrons is assumed (*fittings I*). *Fittings II* are still highly favored in this case (see Table 3).

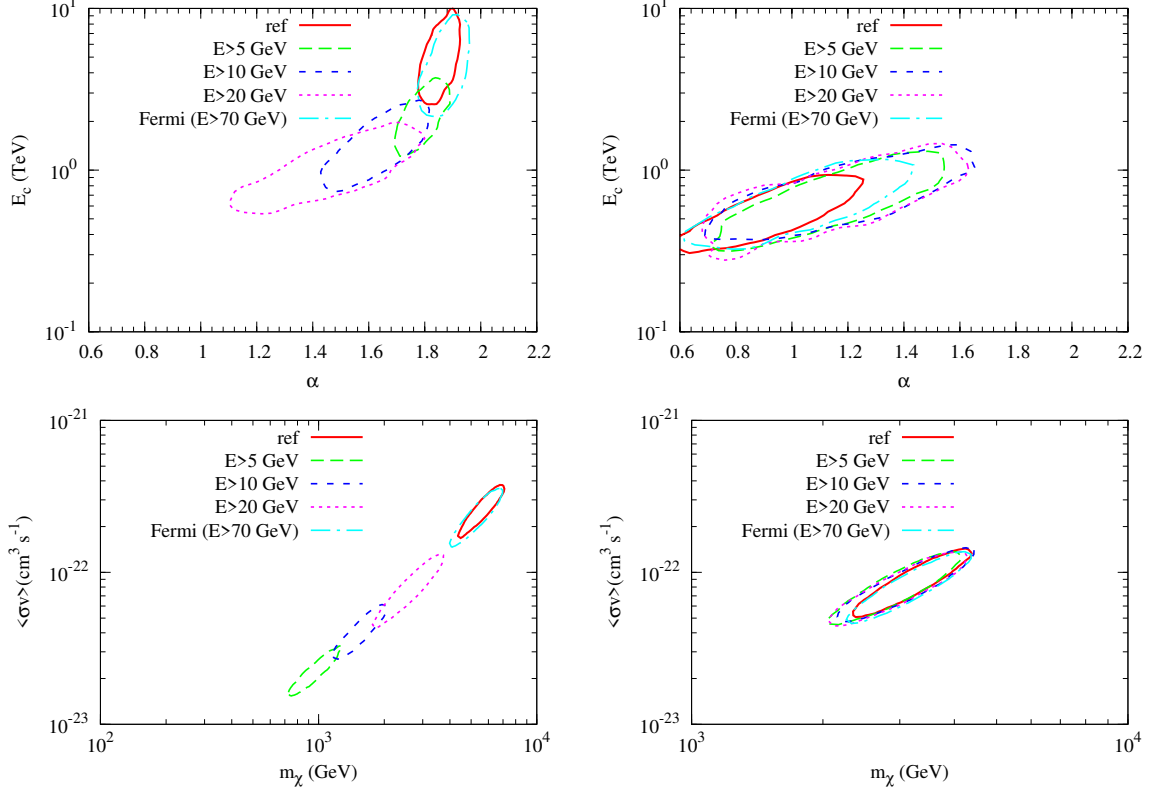


**Figure 3.** Same as Figure 2 but for comparisons of different selections of the low energy data as given in Table 3.

The  $2\sigma$  confidence regions of  $\alpha - E_c$  and  $m_\chi - \langle\sigma v\rangle$  for these fittings are given in Figure 3. It is shown that for *fittings I* the parameter regions differ significantly from each other due to the poor fittings. For *fittings II* the favored parameter regions converge much better for different cases.

### 3.3 Solar modulation

As shown in the last subsection the low energy data are important and may affect the fitting results. However, the low energy CRs are affected by the solar modulation, which still has large uncertainties. Recent works developed three-dimensional, time and charge-sign dependent solar modulation model, HELIOPROP, which can reproduce the low energy spectra of various kinds of species [59]. It has been shown that for the PAMELA data taking time, the force-field approximation gives very similar results to the three-dimensional model, but for the AMS-02 data taking time the force-field approximation may not work well [68]. In this subsection we show how the solar modulation affects the fitting results. For simplicity, we keep in the framework of force-field approximation, but with different choices

of the modulation potentials to partially take into account the effects of different data taking time by different detectors and the difference between the charge-sign.

Through fitting the proton data the modulation potential was estimated to be about 450 to 550 MV during the working period of PAMELA [42]. Such a result has been confirmed by the measurement of the diffuse  $\gamma$ -rays in the solar neighborhood with Fermi-LAT [69, 70]. The periods for electron data taking by PAMELA and Fermi-LAT are almost the same in the solar cycle, thus they should share a common modulation potential as above. In the reference configuration we have taken the solar modulation potential to be independent of the value determined from the proton data. Here we apply a Gaussian prior of  $\phi = 500 \pm 50$  MV on the modulation potential and redo the fitting. As can be seen from Table 4, the fitting  $\chi^2$  values become much larger than that of the reference configuration. In the reference configuration, the best-fitting value of  $\phi$  is about 1000 MV, which differs significantly from the above value induced from the  $\gamma$ -ray and CR nuclei observations. Such a discrepancy may imply that the simple force field approximation may not be enough to describe the solar modulation of all types of CR particles.

**Table 4.** Fitting  $\chi^2/\text{dof}$  for different treatments of the solar modulation.

	ref.	$\phi$ prior	$\phi_1/\phi_2$	$\phi_+/\phi_-$
psr- <i>I</i>	398.2/166	434.8/166	315.6/165	313.5/165
psr- <i>II</i>	134.0/164	227.0/164	127.7/163	135.8/163
DM- <i>I</i>	568.0/167	670.9/167	525.0/166	372.2/166
DM- <i>II</i>	133.9/165	228.6/165	126.7/164	134.3/164

**Table 5.** Mean values and  $1\sigma$  uncertainties of the modulation potentials (in unit of MV) corresponding to different tests in Table 4.

	ref.	$\phi$ prior	$\phi_1/\phi_2$	$\phi_+/\phi_-$
psr- <i>I</i>	$824 \pm 16$	$792 \pm 15$	$691 \pm 20, 1483 \pm 16^a$	$688 \pm 18, 900 \pm 16$
psr- <i>II</i>	$1001 \pm 13$	$965 \pm 14$	$928 \pm 42, 1341 \pm 196^a$	$1060 \pm 103, 1002 \pm 14$
DM- <i>I</i>	$1020 \pm 10$	$998 \pm 10$	$936 \pm 13, 1480 \pm 21^a$	$725 \pm 22, 998 \pm 11$
DM- <i>II</i>	$998 \pm 12$	$974 \pm 11$	$934 \pm 35, 1346 \pm 177^a$	$1044 \pm 110, 999 \pm 13$

<sup>a</sup>Parameter is close to the upper limit 1500 MV of the scan.

Furthermore, considering that the data taking period of PAMELA/Fermi-LAT is different from that of AMS-02, we adopt two potentials,  $\phi_1$  for PAMELA/Fermi-LAT and  $\phi_2$  for AMS-02 to test whether the fittings can be improved. Given one more free parameter, we do have some improvement for *fittings I* compared with the reference model. However, the  $\chi^2$  values are still too large (Table 4). Introducing the spectral hardening of the primary electrons can improve the fittings significantly (*fittings II*). Compared with the reference configuration, the best-fitting  $\chi^2$  values become slightly smaller for *fittings II*. That is to say, a single solar modulation potential seems to work well enough under the present model frame, although adding another modulation potential will improve the fittings slightly. The fitting values of the solar modulation potentials are listed in Table 5. We find that in all these fittings,  $\phi_2 > \phi_1$  is shown, which may reflect the fact that AMS-02 works close to the solar maximum while PAMELA worked during the moderate phase of solar activity.

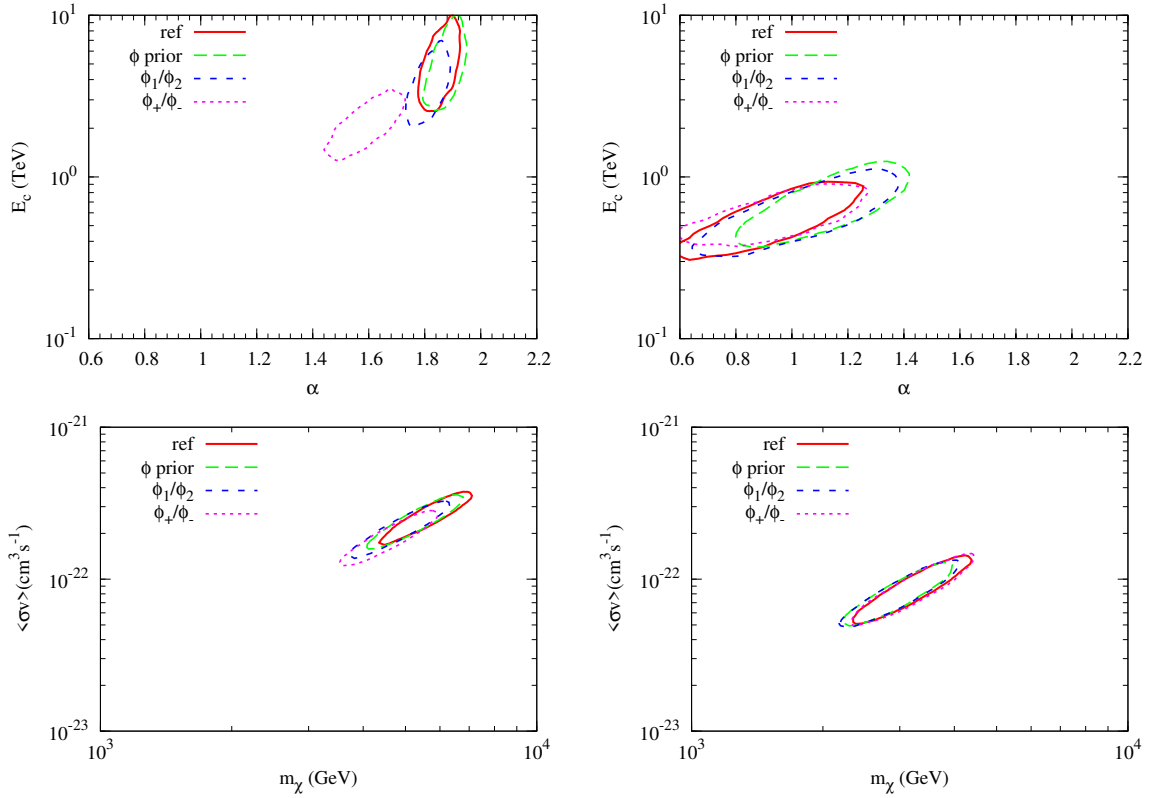


**Figure 4.** Same as Figure 2 but for comparisons of different treatments of the solar modulation as given in Table 4.

Finally, to account for the charge-sign dependent modulation effect, we apply two different modulation potentials,  $\phi_+$  and  $\phi_-$ , on positrons and electrons, respectively. Similar with the  $\phi_1/\phi_2$  scenario, we have some improvement for *fittings I* compared with the reference scenario. However, the improvement is not enough to give a good fitting. For *fittings II*, the best-fitting  $\chi^2$  values are almost the same as the reference configuration, and there is no improvement with an additional free parameter. In addition, we find that  $\phi_+ \approx \phi_-$  for *fittings II* (see Table 5), which indicates that no strong evidence of charge-sign dependent modulation effect is needed from the data.

The confidence regions of the extra source parameters for different treatments of the solar modulation as described above are shown in Figure 4. Similar with the previous cases, we see that for *fittings I* the parameter regions have relatively large dispersion, and for *fittings II* they converge much better.

### 3.4 Other uncertainties

#### 3.4.1 Hadronic interaction model

The hadronic interaction model affects the production spectra of secondary  $e^+e^-$ . In the reference configuration we take the hadronic  $pp$  collision parameterization given in Ref. [71] (K06). As a test we discuss another  $pp$  collision model developed in [72] (D86) which combines isobaric model near the threshold [73] and scaling representations at high energies [74]. This

model is the default hadronic interaction model adopted in the GALPROP package (see Ref. [75] for a detailed description).

The difference of the expected secondary positron fluxes between the two interaction models differs up to several tens of percentages and varies with energy [67]. The fitting results are presented in Table 6 and Figure 5. As can be seen in Table 6, the goodness-of-fit of the D86 model is generally worse than the K06 model, both for *fittings I* and *II*. However, the favored confidence regions of the source parameters, as can be seen in Figure 5, do not differ much from each other.

**Table 6.** Fitting  $\chi^2/\text{dof}$  for other tests.

	ref.	pp-D86	no p hard.	v54
psr-I	398.2/166	505.7/166	359.4/166	367.9/166
psr-II	134.0/164	173.5/164	137.9/164	140.6/164
DM-I	568.0/167	600.3/167	486.8/167	609.0/167
DM-II	133.9/165	175.3/165	137.1/165	140.7/165

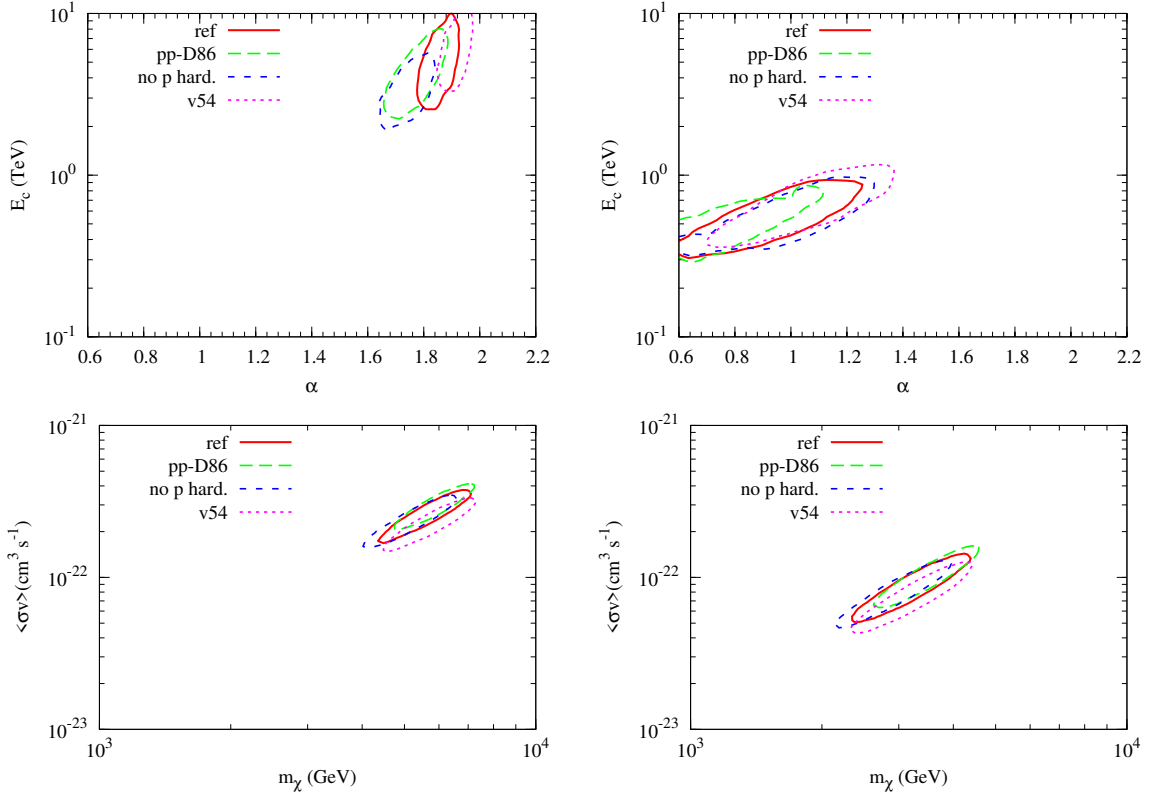


**Figure 5.** Same as Figure 2 but for comparisons of other tests as given in Table 6.

### 3.4.2 Nuclei spectral hardening

The ATIC2, CREAM and PAMELA measurements show that there is a uniform spectral hardening of the CR nuclei spectra at sub-TV rigidities [40–42]. However, the preliminary

data from AMS-02 tend to disfavor the existence of the spectral hardening at  $\sim 200$  GV of the proton and Helium spectra as found by PAMELA [24]. The spectrum of the primary protons will affect the prediction of the secondary positron flux [76]. Therefore we test the case without nuclei spectral hardening here. We fit the propagated proton spectrum to the PAMELA/CREAM data. The fitting  $\chi^2/\text{dof}$  values are 60.1/85 (33.7/84) for the case without (with) nuclei spectral hardening. The differences of the proton spectra, and thus the secondary positron spectra, between these two models are actually very small. We find that the calculated positron flux differ by  $\lesssim 5\%$  at tens of GeV from the reference configuration. It is different from Ref. [76], where the model without the spectral hardening used for comparison was derived through fitting the low energy data only. It is shown from Table 6 that, for *fittings I* the goodness-of-fitting has a little improvement compared with the reference configuration. However, the  $\chi^2$  values are still too large. For *fittings II* the  $\chi^2$  values have almost no change. The confidence regions of the source parameters are very close to that of the reference one, as shown in Figure 5.

### 3.4.3 Versions of GALPROP

For all the previous studies in this work we adopt “v50” of the GALPROP code. A new version “v54” of the code has been developed and made public by the authors in recent years, which has remarkable improvements in several aspects [77]. The most relevant aspect is the update of the interstellar radiation field, which may affect the propagation of leptons. No significant difference of the results between “v50” and “v54” is found<sup>5</sup>. See Table 6 and Figure 5 for the results. Our conclusion obtained based on the “v50” version code should not be affected given the new version of the propagation code.

## 4 Discussion about the electron spectral hardening

From all the above tests, an additional spectral hardening of the primary electron spectrum at  $O(100)$  GV is strongly favored in order to fit the  $e^+e^-$  data from  $\sim\text{GeV}$  to  $\sim\text{TeV}$  simultaneously. A natural explanation of the spectral hardening could be the discreteness of the CR sources [45–47]. Since the effective propagation length of TeV electrons within the cooling time of TeV electrons, which is  $O(10^5)$  yrs, is  $\lesssim$  kpc [52], the number of CR sources which can contribute to the local electrons, e.g. supernova remnants, is very small. Thus it is likely that one or few nearby sources contribute more significant to the high energy part of the electron spectrum and result in a harder spectrum than the background extension [45–47].

The fitting under the assumption of continuous CR source distribution seems indicating the importance of local sources. However, it will be impossible to incorporate all the discrete sources in the global fitting procedure, since there will be too many free parameters in that case. The continuous source assumption could be regarded as the average of a randomly assigned CR source distribution. The deviation from this average result may directly indicate the break down of the continuous source assumption. The studies taking into account the discrete distribution of sources can be found in Refs. [28, 47, 52].

Alternatively, other mechanisms proposed to explain the CR nuclei hardening, such as the superposition of multiple components of sources [78, 79], the change of injection spectrum due to non-linear acceleration process [80], the propagation effect [81–83] etc. (see [84] for a compilation and implication of these different types of models), may also apply for the

<sup>5</sup>Here we adopt version 54.1.984 of the code. The latest updated version can be obtained at <http://sourceforge.net/projects/galprop/>

electrons. However, the hardening of the electrons seems to be much more significant than that of nuclei, which may challenge some of the models.

Another possibility is that the contributions to positrons and electrons from the extra sources are non-equal, i.e., there is a charge asymmetry of the extra sources. It can be realized in the asymmetric DM scenario within the  $R$ -parity violation supersymmetry framework [43].

## 5 Conclusion

In this work we give a systematic study on the uncertainties of fitting the CR  $e^+e^-$  data. The potential sources of the uncertainties discussed include the CR propagation, the selection of low energy data, the solar modulation, the hadronic interaction model, the spectral hardening of nuclei and the versions of the propagation code. The major conclusions are summarized as follows.

- In general a spectral hardening of the background electron spectrum is favored, in spite that there are various kinds of uncertainties from the CR propagation and the solar modulation. The break energy is about 50 – 100 GeV, and the change of the spectral index is about 0.3 – 0.4. The required spectral hardening may indicate the contributions to high energy electrons from nearby CR sources. In this case the continuous assumption of the source distribution will break down and the fluctuation from discrete source(s) dominate the high energy behavior of the primary electrons.
- The propagation models and parameters lead to one of the main uncertainties of the fittings. Varying the propagation parameters in a wide range allowed by the present CR data will make the constraints on the  $e^+e^-$  extra source parameters loosen by a factor of  $\sim 2$ .
- The exclusion of low energy data will affect the results of the fittings. If the low energy data below tens of GeV are excluded in the fittings, the AMS-02/Fermi data can be fitted without introducing an electron spectral hardening. This is because only the high energy spectral behavior is constrained by the data. Such a conclusion based on the fitting to the high energy data only may be biased.
- The solar modulation does not affect the fitting results much, although it does lead to uncertainties in the modeling of the low energy spectra. The modulation potential for  $e^+e^-$  is usually greater than that for protons.
- The hadronic interaction models, the proton spectral hardening and the propagation code versions have very small effects in the results.
- For fittings with large  $\chi^2$  values (*fittings I* and few cases in *fittings II*) the derived source parameters have very large dispersion, while for the fittings with acceptable  $\chi^2$  values the parameter regions converge very well for different model settings. For the pulsar scenario, the spectral index  $\alpha \sim 1$  and the cutoff energy  $E_c \sim 0.5$  TeV are found, and for the DM annihilation into a pair of taus,  $m_\chi \sim 3$  TeV and  $\langle\sigma v\rangle \sim 6 \times 10^{-23}$  cm<sup>3</sup>s<sup>-1</sup> are favored.

## Acknowledgments

We thank the anonymous referee for helpful comments and suggestions which improve this paper much. This work is supported by 973 Program under Grant No. 2013CB837000, and by National Natural Science Foundation of China under Grant Nos. 11135009, 11105155 and by the Strategic Priority Research Program “The Emergence of Cosmological Structures” of the Chinese Academy of Sciences under Grant No. XDB09000000.

## Appendix: Results for different annihilation channel of DM

Here we present the fitting contours on the  $m_\chi - \langle\sigma v\rangle$  plane for DM annihilation channels  $\mu^+\mu^-$ ,  $\tau^+\tau^-$ ,  $4e$ ,  $4\mu$  and  $4\tau$ , respectively. For the  $4e$ ,  $4\mu$  and  $4\tau$  channels we assume the mass of the intermediate particle  $\phi$  is 100 GeV. The other settings are the same as the reference configuration plus a high energy spectral hardening of the primary electrons as presented in Sec. 2.

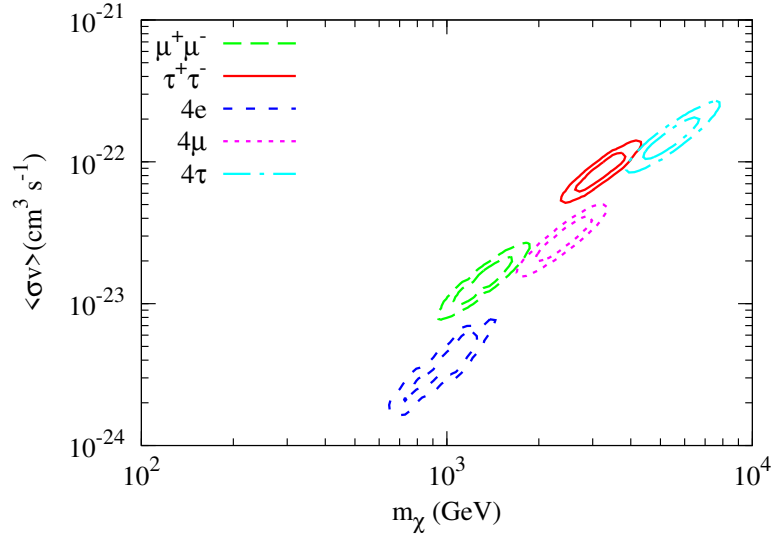


**Figure 6.** 1 and  $2\sigma$  fitting contours on the  $m_\chi - \langle\sigma v\rangle$  plane for different DM annihilation channels.

## References

- [1] S. W. Barwick, et al., *Measurements of the Cosmic-Ray Positron Fraction from 1 to 50 GeV*, *Astrophys. J. Lett.* **482** (June, 1997) L191, [[astro-ph/9703192](#)].
- [2] M. Aguilar, et al., *Cosmic-ray positron fraction measurement from 1 to 30 GeV with AMS-01*, *Phys. Lett. B* **646** (Mar., 2007) 145–154, [[astro-ph/0703154](#)].
- [3] O. Adriani, et al., *An anomalous positron abundance in cosmic rays with energies 1.5-100 GeV*, *Nature* **458** (Apr., 2009) 607–609, [[arXiv:0810.4995](#)].
- [4] O. Adriani, et al., *A statistical procedure for the identification of positrons in the PAMELA experiment*, *Astroparticle Physics* **34** (Aug., 2010) 1–11, [[arXiv:1001.3522](#)].
- [5] M. Aguilar, et al., *First result from the Alpha Magnetic Spectrometer on the International Space Station: precision measurement of the positron fraction in primary cosmic rays of 0.5-350 GeV*, *Phys. Rev. Lett.* **110** (Apr., 2013) 141102.



- [6] P. D. Serpico, *Possible causes of a rise with energy of the cosmic ray positron fraction*, *Phys. Rev. D* **79** (Jan., 2009) 021302, [[arXiv:0810.4846](#)].
- [7] I. V. Moskalenko, *Cosmic Rays in the Milky Way and Beyond*, *Nuclear Physics B Proceedings Supplements* **243** (Oct., 2013) 85–91, [[arXiv:1308.5482](#)].
- [8] X. He, *Dark Matter Annihilation Explanation for  $e^\pm$  Excesses in Cosmic Ray*, *Modern Physics Letters A* **24** (2009) 2139–2160, [[arXiv:0908.2908](#)].
- [9] Y.-Z. Fan, B. Zhang, and J. Chang, *Electron/positron Excesses in the Cosmic Ray Spectrum and Possible Interpretations*, *International Journal of Modern Physics D* **19** (2010) 2011–2058, [[arXiv:1008.4646](#)].
- [10] P. D. Serpico, *Astrophysical models for the origin of the positron "excess"*, *Astroparticle Physics* **39** (Dec., 2012) 2–11, [[arXiv:1108.4827](#)].
- [11] M. Cirelli, *Indirect searches for dark matter*, *Pramana* **79** (Nov., 2012) 1021–1043, [[arXiv:1202.1454](#)].
- [12] X.-J. Bi, P.-F. Yin, and Q. Yuan, *Status of dark matter detection*, *Frontiers of Physics* **8** (Dec., 2013) 794–827, [[arXiv:1409.4590](#)].
- [13] J. Liu, Q. Yuan, X. J. Bi, H. Li, and X. M. Zhang, *Markov chain Monte Carlo study on dark matter property related to the cosmic  $e^\pm$  excesses*, *Phys. Rev. D* **81** (Jan., 2010) 023516, [[arXiv:0906.3858](#)].
- [14] J. Liu, Q. Yuan, X.-J. Bi, H. Li, and X. Zhang, *Cosmic ray Monte Carlo: A global fitting method in studying the properties of the new sources of cosmic  $e^\pm$  excesses*, *Phys. Rev. D* **85** (Feb., 2012) 043507, [[arXiv:1106.3882](#)].
- [15] Q. Yuan, X.-J. Bi, G.-M. Chen, Y.-Q. Guo, S.-J. Lin, and X. Zhang, *Implications of the AMS-02 positron fraction in cosmic rays*, *Astroparticle Physics* **60** (Jan., 2015) 1–12, [[arXiv:1304.1482](#)].
- [16] O. Adriani, et al., *Cosmic-Ray Electron Flux Measured by the PAMELA Experiment between 1 and 625 GeV*, *Phys. Rev. Lett.* **106** (May, 2011) 201101, [[arXiv:1103.2880](#)].
- [17] A. A. Abdo, et al., *Measurement of the Cosmic Ray  $e^+ + e^-$  Spectrum from 20 GeV to 1 TeV with the Fermi Large Area Telescope*, *Phys. Rev. Lett.* **102** (May, 2009) 181101, [[arXiv:0905.0025](#)].
- [18] M. Ackermann, et al., *Fermi LAT observations of cosmic-ray electrons from 7 GeV to 1 TeV*, *Phys. Rev. D* **82** (Nov., 2010) 092004, [[arXiv:1008.3999](#)].
- [19] F. Aharonian, et al., *Energy Spectrum of Cosmic-Ray Electrons at TeV Energies*, *Phys. Rev. Lett.* **101** (Dec., 2008) 261104, [[arXiv:0811.3894](#)].
- [20] F. Aharonian, et al., *Probing the ATIC peak in the cosmic-ray electron spectrum with H.E.S.S.*, *Astron. Astrophys.* **508** (Dec., 2009) 561–564, [[arXiv:0905.0105](#)].
- [21] I. Cholis and D. Hooper, *Dark matter and pulsar origins of the rising cosmic ray positron fraction in light of new data from the AMS*, *Phys. Rev. D* **88** (July, 2013) 023013, [[arXiv:1304.1840](#)].
- [22] I. Masina and F. Sannino, *Hints of a charge asymmetry in the electron and positron cosmic-ray excesses*, *Phys. Rev. D* **87** (June, 2013) 123003, [[arXiv:1304.2800](#)].
- [23] H.-B. Jin, Y.-L. Wu, and Y.-F. Zhou, *Implications of the first AMS-02 measurement for dark matter annihilation and decay*, *JCAP* **11** (Nov., 2013) 26, [[arXiv:1304.1997](#)].
- [24] AMS-02 collaboration, , in *International Cosmic Ray Conference*, <http://www.ams02.org/2013/07/new-results-from-ams-presented-at-icrc-2013/>, 2013.

- [25] G. di Bernardo, C. Evoli, D. Gaggero, D. Grasso, and L. Maccione, *Unified interpretation of cosmic ray nuclei and antiproton recent measurements*, *Astroparticle Physics* **34** (Dec., 2010) 274–283, [[arXiv:0909.4548](#)].
- [26] R. Trotta, G. Jóhannesson, I. V. Moskalenko, T. A. Porter, R. Ruiz de Austri, and A. W. Strong, *Constraints on Cosmic-ray Propagation Models from A Global Bayesian Analysis*, *Astrophys. J.* **729** (Mar., 2011) 106, [[arXiv:1011.0037](#)].
- [27] L. Feng, R.-Z. Yang, H.-N. He, T.-K. Dong, Y.-Z. Fan, and J. Chang, *AMS-02 positron excess: New bounds on dark matter models and hint for primary electron spectrum hardening*, *Physics Letters B* **728** (Jan., 2014) 250–255, [[arXiv:1303.0530](#)].
- [28] T. Linden and S. Profumo, *Probing the Pulsar Origin of the Anomalous Positron Fraction with AMS-02 and Atmospheric Cherenkov Telescopes*, *Astrophys. J.* **772** (July, 2013) 18, [[arXiv:1304.1791](#)].
- [29] D. Gaggero and L. Maccione, *Model independent interpretation of recent CR lepton data after AMS-02*, *JCAP* **12** (Dec., 2013) 11, [[arXiv:1307.0271](#)].
- [30] M. Ibe, S. Matsumoto, S. Shirai, and T. T. Yanagida, *AMS-02 positrons from decaying Wino in the pure gravity mediation model*, *Journal of High Energy Physics* **7** (July, 2013) 63, [[arXiv:1305.0084](#)].
- [31] D. Malyshev, I. Cholis, and J. Gelfand, *Pulsars versus dark matter interpretation of ATIC/PAMELA*, *Phys. Rev. D* **80** (Sept., 2009) 063005, [[arXiv:0903.1310](#)].
- [32] N. Kawanaka, K. Ioka, and M. M. Nojiri, *Is Cosmic Ray Electron Excess from Pulsars Spiky or Smooth?: Continuous and Multiple Electron/Positron Injections*, *Astrophys. J.* **710** (Feb., 2010) 958–963, [[arXiv:0903.3782](#)].
- [33] D. Hooper, A. Stebbins, and K. M. Zurek, *Excesses in cosmic ray positron and electron spectra from a nearby clump of neutralino dark matter*, *Phys. Rev. D* **79** (May, 2009) 103513, [[arXiv:0812.3202](#)].
- [34] M. Kuhlen and D. Malyshev, *ATIC, PAMELA, HESS, and Fermi data and nearby dark matter subhalos*, *Phys. Rev. D* **79** (June, 2009) 123517, [[arXiv:0904.3378](#)].
- [35] J. Lavalle, Q. Yuan, D. Maurin, and X. Bi, *Full calculation of clumpiness boost factors for antimatter cosmic rays in the light of  $\Lambda$ CDM  $N$ -body simulation results. Abandoning hope in clumpiness enhancement?*, *Astron. Astrophys.* **479** (Feb., 2008) 427–452, [[arXiv:0709.3634](#)].
- [36] P. Brun, T. Delahaye, J. Diemand, S. Profumo, and P. Salati, *Cosmic ray lepton puzzle in the light of cosmological  $N$ -body simulations*, *Phys. Rev. D* **80** (Aug., 2009) 035023, [[arXiv:0904.0812](#)].
- [37] Q. Yuan and X.-J. Bi, *Reconcile the AMS-02 positron fraction and Fermi-LAT/HESS total  $e$  spectra by the primary electron spectrum hardening*, *Physics Letters B* **727** (Nov., 2013) 1–7, [[arXiv:1304.2687](#)].
- [38] A. W. Strong and I. V. Moskalenko, *Propagation of Cosmic-Ray Nucleons in the Galaxy*, *Astrophys. J.* **509** (Dec., 1998) 212–228, [[astro-ph/9807150](#)].
- [39] A. W. Strong, E. Orlando, and T. R. Jaffe, *The interstellar cosmic-ray electron spectrum from synchrotron radiation and direct measurements*, *Astron. Astrophys.* **534** (Oct., 2011) A54, [[arXiv:1108.4822](#)].
- [40] A. D. Panov, et al., *Elemental energy spectra of cosmic rays from the data of the ATIC-2 experiment*, *Bulletin of the Russian Academy of Science, Phys.* **71** (Apr., 2007) 494–497, [[astro-ph/0612377](#)].
- [41] H. S. Ahn, et al., *Discrepant Hardening Observed in Cosmic-ray Elemental Spectra*, *Astrophys. J. Lett.* **714** (May, 2010) L89–L93, [[arXiv:1004.1123](#)].

- [42] O. Adriani, et al., *PAMELA Measurements of Cosmic-Ray Proton and Helium Spectra*, *Science* **332** (Apr., 2011) 69–, [[arXiv:1103.4055](#)].
- [43] L. Feng and Z. Kang, *Decaying asymmetric dark matter relaxes the AMS-Fermi tension*, *JCAP* **10** (Oct., 2013) 8, [[arXiv:1304.7492](#)].
- [44] C.-Q. Geng, D. Huang, and L.-H. Tsai, *Imprint of multicomponent dark matter on AMS-02*, *Phys. Rev. D* **89** (Mar., 2014) 055021, [[arXiv:1312.0366](#)].
- [45] G. Bernard, T. Delahaye, Y.-Y. Keum, W. Liu, P. Salati, and R. Taillet, *TeV cosmic-ray proton and helium spectra in the myriad model*, *Astron. Astrophys.* **555** (July, 2013) A48, [[arXiv:1207.4670](#)].
- [46] S. Thoudam and J. R. Hörandel, *Nearby supernova remnants and the cosmic ray spectral hardening at high energies*, *Mon. Not. Roy. Astron. Soc.* **421** (Apr., 2012) 1209–1214, [[arXiv:1112.3020](#)].
- [47] M. Di Mauro, F. Donato, N. Fornengo, R. Lineros, and A. Vittino, *Interpretation of AMS-02 electrons and positrons data*, *JCAP* **4** (Apr., 2014) 6, [[arXiv:1402.0321](#)].
- [48] M. Cirelli, M. Kadastik, M. Raidal, and A. Strumia, *Model-independent implications of the  $e^\pm$ ,  $\bar{p}$  cosmic ray spectra on properties of Dark Matter*, *Nuclear Physics B* **813** (May, 2009) 1–21, [[arXiv:0809.2409](#)].
- [49] C.-Y. Huang, S.-E. Park, M. Pohl, and C. D. Daniels, *Gamma-rays produced in cosmic-ray interactions and the TeV-band spectrum of RX J1713.7-3946*, *Astroparticle Physics* **27** (June, 2007) 429–439, [[astro-ph/0611854](#)].
- [50] D. R. Lorimer, *The Galactic Population and Birth Rate of Radio Pulsars*, in *Young Neutron Stars and Their Environments* (F. Camilo & B. M. Gaensler, ed.), vol. 218 of *IAU Symposium*, p. 105, 2004.
- [51] A. A. Abdo, et al., *The Second Fermi Large Area Telescope Catalog of Gamma-Ray Pulsars*, *Astrophys. J. Suppl.* **208** (Oct., 2013) 17, [[arXiv:1305.4385](#)].
- [52] P.-F. Yin, Z.-H. Yu, Q. Yuan, and X.-J. Bi, *Pulsar interpretation for the AMS-02 result*, *Phys. Rev. D* **88** (July, 2013) 023001, [[arXiv:1304.4128](#)].
- [53] O. Adriani, et al., *PAMELA Results on the Cosmic-Ray Antiproton Flux from 60 MeV to 180 GeV in Kinetic Energy*, *Phys. Rev. Lett.* **105** (Sept., 2010) 121101, [[arXiv:1007.0821](#)].
- [54] F. Donato, D. Maurin, P. Brun, T. Delahaye, and P. Salati, *Constraints on WIMP Dark Matter from the High Energy PAMELA  $\bar{p}/p$  Data*, *Phys. Rev. Lett.* **102** (Feb., 2009) 071301, [[arXiv:0810.5292](#)].
- [55] P. Meade, M. Papucci, A. Strumia, and T. Volansky, *Dark Matter interpretations of the  $e^\pm$  excesses after FERMI*, *Nuclear Physics B* **831** (May, 2010) 178–203, [[arXiv:0905.0480](#)].
- [56] J. F. Navarro, C. S. Frenk, and S. D. M. White, *A Universal Density Profile from Hierarchical Clustering*, *Astrophys. J.* **490** (Dec., 1997) 493, [[astro-ph/9611107](#)].
- [57] L. J. Gleeson and W. I. Axford, *Solar Modulation of Galactic Cosmic Rays*, *Astrophys. J.* **154** (Dec., 1968) 1011.
- [58] S. Della Torre, et al., *Effects of solar modulation on the cosmic ray positron fraction*, *Advances in Space Research* **49** (June, 2012) 1587–1592.
- [59] L. Maccione, *Low Energy Cosmic Ray Positron Fraction Explained by Charge-Sign Dependent Solar Modulation*, *Phys. Rev. Lett.* **110** (Feb., 2013) 081101, [[arXiv:1211.6905](#)].
- [60] J. M. Clem, D. P. Clements, J. Esposito, P. Evenson, D. Huber, J. L’Heureux, P. Meyer, and C. Constantin, *Solar Modulation of Cosmic Electrons*, *Astrophys. J.* **464** (June, 1996) 507.

- [61] B. Beischer, P. von Doetinchem, H. Gast, T. Kirn, and S. Schael, *Perspectives for indirect dark matter search with AMS-2 using cosmic-ray electrons and positrons*, *New Journal of Physics* **11** (Oct., 2009) 105021.
- [62] I. V. Moskalenko, A. W. Strong, J. F. Ormes, and M. S. Potgieter, *Secondary Antiprotons and Propagation of Cosmic Rays in the Galaxy and Heliosphere*, *Astrophys. J.* **565** (Jan., 2002) 280–296, [[astro-ph/0106567](#)].
- [63] A. W. Strong, I. V. Moskalenko, and O. Reimer, *Diffuse Galactic Continuum Gamma Rays: A Model Compatible with EGRET Data and Cosmic-Ray Measurements*, *Astrophys. J.* **613** (Oct., 2004) 962–976, [[astro-ph/0406254](#)].
- [64] M. Ackermann, et al., *Constraints on the Galactic Halo Dark Matter from Fermi-LAT Diffuse Measurements*, *Astrophys. J.* **761** (Dec., 2012) 91, [[arXiv:1205.6474](#)].
- [65] P. F. Yin, Q. Yuan, J. Liu, J. Zhang, X. J. Bi, S. H. Zhu, and X. M. Zhang, *PAMELA data and leptonically decaying dark matter*, *Phys. Rev. D* **79** (Jan., 2009) 023512, [[arXiv:0811.0176](#)].
- [66] A. Putze, L. Derome, and D. Maurin, *A Markov Chain Monte Carlo technique to sample transport and source parameters of Galactic cosmic rays. II. Results for the diffusion model combining B/C and radioactive nuclei*, *Astron. Astrophys.* **516** (June, 2010) A66, [[arXiv:1001.0551](#)].
- [67] T. Delahaye, R. Lineros, F. Donato, N. Fornengo, J. Lavalle, P. Salati, and R. Taillet, *Galactic secondary positron flux at the Earth*, *Astron. Astrophys.* **501** (July, 2009) 821–833, [[arXiv:0809.5268](#)].
- [68] D. Gaggero, L. Maccione, D. Grasso, G. Di Bernardo, and C. Evoli, *PAMELA and AMS-02  $e^+$  and  $e^-$  spectra are reproduced by three-dimensional cosmic-ray modeling*, *Phys. Rev. D* **89** (Apr., 2014) 083007, [[arXiv:1311.5575](#)].
- [69] A. A. Abdo, et al., *Fermi LAT Observation of Diffuse Gamma Rays Produced Through Interactions Between Local Interstellar Matter and High-energy Cosmic Rays*, *Astrophys. J.* **703** (Oct., 2009) 1249–1256, [[arXiv:0908.1171](#)].
- [70] J.-M. Casandjian, , in *International Cosmic Ray Conference*, [www.cbpf.br/~icrc2013/papers/icrc2013-0966.pdf](http://www.cbpf.br/~icrc2013/papers/icrc2013-0966.pdf), 2013.
- [71] T. Kamae, N. Karlsson, T. Mizuno, T. Abe, and T. Koi, *Parameterization of  $\gamma$ ,  $e^{+/-}$ , and Neutrino Spectra Produced by p-p Interaction in Astronomical Environments*, *Astrophys. J.* **647** (Aug., 2006) 692–708, [[astro-ph/0605581](#)].
- [72] C. D. Dermer, *Binary collision rates of relativistic thermal plasmas. II - Spectra*, *Astrophys. J.* **307** (Aug., 1986) 47–59.
- [73] F. W. Stecker, *The Cosmic  $\gamma$ -Ray Spectrum from Secondary Particle Production in Cosmic-Ray Interactions*, *Astrophys. Space Sci.* **6** (Mar., 1970) 377–389.
- [74] G. D. Badhwar, R. L. Golden, and S. A. Stephens, *Analytic representation of the proton-proton and proton-nucleus cross-sections and its application to the sea-level spectrum and charge ratio of muons*, *Phys. Rev. D* **15** (Feb., 1977) 820–831.
- [75] I. V. Moskalenko and A. W. Strong, *Production and Propagation of Cosmic-Ray Positrons and Electrons*, *Astrophys. J.* **493** (Jan., 1998) 694, [[astro-ph/9710124](#)].
- [76] J. Lavalle, *Impact of the spectral hardening of TeV cosmic rays on the prediction of the secondary positron flux*, *Mon. Not. Roy. Astron. Soc.* **414** (June, 2011) 985–991, [[arXiv:1011.3063](#)].
- [77] A. W. Strong, I. V. Moskalenko, T. A. Porter, G. Jóhannesson, E. Orlando, and S. W. Digel, *The GALPROP Cosmic-Ray Propagation Code*, *ArXiv e-prints* (July, 2009) [[arXiv:0907.0559](#)].

- [78] Q. Yuan, B. Zhang, and X.-J. Bi, *Cosmic ray spectral hardening due to dispersion in the source injection spectra*, *Phys. Rev. D* **84** (Aug., 2011) 043002, [[arXiv:1104.3357](#)].
- [79] A. D. Erlykin and A. W. Wolfendale, *A New Component of Cosmic Rays?*, *Astroparticle Physics* **35** (Jan., 2012) 449–456, [[arXiv:1111.3191](#)].
- [80] V. Ptuskin, V. Zirakashvili, and E.-S. Seo, *Spectra of Cosmic-Ray Protons and Helium Produced in Supernova Remnants*, *Astrophys. J.* **763** (Jan., 2013) 47, [[arXiv:1212.0381](#)].
- [81] N. Tomassetti, *Origin of the Cosmic-Ray Spectral Hardening*, *Astrophys. J. Lett.* **752** (June, 2012) L13, [[arXiv:1204.4492](#)].
- [82] P. Blasi, E. Amato, and P. D. Serpico, *Spectral Breaks as a Signature of Cosmic Ray Induced Turbulence in the Galaxy*, *Physical Review Letters* **109** (Aug., 2012) 061101, [[arXiv:1207.3706](#)].
- [83] S. Thoudam and J. R. Hörandel, *GeV-TeV cosmic-ray spectral anomaly as due to reacceleration by weak shocks in the Galaxy*, *Astron. Astrophys.* **567** (July, 2014) A33, [[arXiv:1404.3630](#)].
- [84] A. E. Vladimirov, G. Jóhannesson, I. V. Moskalenko, and T. A. Porter, *Testing the Origin of High-energy Cosmic Rays*, *Astrophys. J.* **752** (June, 2012) 68, [[arXiv:1108.1023](#)].